2024-06-07

MEDIAL TEMPORAL LOBE SURFACE FEATURES AND COGNITION IN AGING AMYLOID-POSITIVE INDIVIDUALS

Jacob Johnston

Honors Thesis

MEDIAL TEMPORAL LOBE SURFACE FEATURES AND COGNITION IN AGING AMYLOID-POSITIVE INDIVIDUALS

by
Jacob Johnston

Submitted to Brigham Young University in partial fulfillment of graduation requirements for University Honors

Neuroscience Center
Brigham Young University
June 2024

Advisor: Derin Cobia

Honors Coordinator: Rebekka Matheson

ABSTRACT

MEDIAL TEMPORAL LOBE SURFACE FEATURES AND COGNITION IN AGING AMYLOID-POSITIVE INDIVIDUALS

Jacob Johnston

Neuroscience Center

Bachelor of Science

Memory consolidation and metabolism are known to differ between amyloid-beta plaque positive (A+) and negative (A-) amnestic Mild Cognitive Impairment (aMCI) and Alzheimer's disease (AD) dementia participants despite similar medial temporal lobe (MTL) volume between groups. Using high-dimensional surface analysis (shape characterization), this study identified structural differences in the medial temporal lobe between A+ aMCI, A+ AD dementia, and amyloid-negative (A-) healthy control groups (CON), specifically in the CA1 and subiculum regions of the hippocampus and entorhinal cortex. Additionally, regional brain surface-based features were correlated with procedural and episodic memory measures, finding positive associations between CA1 integrity and episodic memory in both A+ participant groups, and a negative correlation between CA1 and procedural memory retention specifically in aMCI participants. The entorhinal cortex also showed correlations with episodic and procedural learning in AD.

TABLE OF CONTENTS

LIST OF FIGURES AND TABLES

Introduction

Alzheimer's Disease (AD) is the most prevalent form of age-related neurodegenerative disease. It is estimated that 6.5 million Americans currently live with the disease, with that number projected to reach 8.5 million by 2030 ("2023 Alzheimer's Disease Facts and Figures," 2023). AD results in progressive loss of memory, cognitive function, motor control, and, ultimately, organ function. There are many clinical markers and biomarkers required for an AD diagnosis, although neuropathology can only confirm diagnosis upon an FDG-PET scan or postmortem autopsy (Jack et al., 2018).

Amyloid-beta plaque (A+), tau (neurofibrillary) tangle(T+), and neurodegenerative (N+) biomarkers are the three most-strongly implicated pathological biomarkers for AD to the field's current knowledge (Jack et al., 2018). Both A+ and T+ patients have demonstrated memory loss in AD correlated with cortical atrophy (N+) (Jahn, 2013). A+/T+ biomarkers often emerge prior to the development of cognitive impairment or cortical atrophy (Villemagne et al., 2013), suggesting a possible causal mechanism for neurodegeneration; some research claims amyloid positivity is the main cause of AD pathology (Hardy & Higgins, 1992), while other research credits the accumulation of neurofibrillary (tau) tangles (Giacobini & Gold, 2013). No consensus has been reached in favor of either claim, leaving room for additional exploration.

The prevalence of A/T/N biomarker positivity increases with age, and, according to a study by Jack et al. (2017), the most prevalent combination in both men and women before the age of 80 is A-/T-/N-. However, by the age of 80 the most common combination is A+/T+/N+, indicating a significant increase in AD pathology as people age (Jack et al., 2017).

Few A/T/N-focused studies to date have reported race or ethnicity of participants, despite the fact that Black (19%) and Hispanic (14%) populations are significantly more likely than White (10%) populations to develop AD across their lifetimes (Rajan et al., 2021). Thus, the A/T/N classification still must be tested amongst diverse populations to test its generalizability. For example, Honig and colleagues (2023) found the A/T/N classification system to be an effective predictor of AD in an ethnically Caribbean-Hispanic cohort.

Women are more likely to develop AD and experience greater symptom severity compared to men (Long et al., 2023). It has been shown that men and women have distinct pathology in AD progression, with women having a higher T+ load as compared to men with AD symptomology and pathology (Oveisgharan et al., 2018). Another study showed no difference in A+ between the sexes (Ferretti et al., 2018), though other studies have found women to have elevated amyloid load compared to men with similar levels of cognitive impairment (Roberts et al., 2018). However, the exact nature of these sex differences is still under investigation.

Many hypotheses have identified various other possible geneses of or contributing factors to AD pathology, such as cardiovascular or cerebrovascular integrity (Bracko et al., 2021; Saeed et al., 2023) or glycolytic efficiency (Goyal et al., 2023; Saito et al., 2022), but research is ongoing and inconclusive.

Despite the uncertainty of pathological causes, the medial temporal lobe (which includes the hippocampal formation, entorhinal cortex, and parahippocampal gyrus) has been definitively shown to be the primary target of neurodegeneration in patients with AD pathology (Chauveau et al., 2021), indicating its significance in understanding the

initiation and progression of AD pathology. Most studies of AD have focused on total-volume atrophy of these regions, but newer tools have given researchers the ability to characterize more subtle cortical and subcortical changes, affording a more complete characterization of the brain, which is called “morphometry” (A. R. Khan et al., 2008).

The aim of this study is to utilize surface-based imaging measures to characterize the morphometry of MTL structures in AD. Morphometric or morphologic characterization is an advanced imaging procedure that has demonstrated increased sensitivity to subtle changes in the brain as a result of neurologic and psychiatric disease compared to gross volumetric analysis (Csernansky, Hamstra, et al., 2004). Previous studies have begun the work of characterizing AD through this methodology and provide promising results for detection of novel pathological processes in AD and aMCI, such as increased gyrification of the entorhinal cortex and hippocampal shape deformation spanning across subregions (Núñez et al., 2020; Zheng et al., 2023). Such sensitivity to atrophy patterns motivates the use of morphometry in this study. Furthermore, relating shape features with cognitive or memory measures improves understanding of functional anatomy and may provide enhanced diagnostic capability for clinicians as the field evolves.

Human memory systems consist of two different categories: declarative and implicit. Declarative memory is the consolidation and retention of events and facts, and consists of semantic and episodic memory. Implicit memory has many subtypes, a major subtype being procedural memory, which is the retention of motor-related actions and habits and the focus of the current study (Kropotov, 2009). Episodic memory is primarily affected in AD and is correlated very strongly with MTL integrity (Eichenbaum &

Lipton, 2008). In the famous case study of patient H.M., bilateral loss of temporal lobe resulted in a complete anterograde amnesia and partial retrograde amnesia, providing initial evidence of the MTL as the primary episodic memory consolidation center (Scoville & Milner, 1957). In contrast, procedural memory is relatively retained through the early- to mid-stages of the disease (Beaunieux et al., 2012; Keith et al., 2023), and has distinct neural circuitry. Though largely different in circuitry and anatomical correlation, the two memory systems share some common brain structures including some portions of the MTL and the prefrontal cortex.

Because MTL integrity has a strong relationship with episodic memory consolidation, it might be expected that MTL volume and memory follow a consistent linear pattern in all disease cohorts. However, a recent finding from our collaborative group (Haut, et al., under review) indicates differential episodic memory retention in A+ versus A- participants despite no difference in MTL volume between groups, suggesting the presence of other potential MTL mechanisms between A+ and A- groups that are not captured by volumetric analysis alone. Thus, utilizing alternative morphometric procedures to characterize the MTL distinctions in A+ patients is a primary focus of this study. This also creates the opportunity for additional investigation to characterize MTL cortical deformations in A- populations.

For research purposes, the literature has classified persons with AD pathology into three broad categories that have many proposed subcategories, primarily based upon progressively more serious cognitive symptoms: preclinical AD, Mild Cognitive Impairment (MCI), and dementia due to Alzheimer's disease (AD dementia) ("2023 Alzheimer's Disease Facts and Figures," 2023). Patients often progress from preclinical

AD to MCI to AD dementia, but progression is not guaranteed with biomarker-positive patients (Parnetti et al., 2019). Because biomarkers are present early in disease progression, many recent publications have focused on preclinical AD and MCI patient groups with the goal of understanding pathological progression of the disease, which will allow for earlier therapeutic intervention and potentially extend the functional lifespan of patients. The current study included amnestic MCI (aMCI) participants in addition to AD dementia participants to represent this early trajectory of AD, and sought to characterize the differences between those with AD pathological biomarkers (A+) and healthy controls.

The current work is based on the evidence-supported claim that the hippocampus is the brain's memory center, and that neuronal amyloidosis is a strong predictive biomarker for probable AD pathology. Illustration of relationships between limbic structures, beta-amyloid plaque presence, and cognitive and memory performance will advance understanding of AD pathological progression. The current study will provide further evidence to the beta-amyloid hypothesis debate and context for therapeutic interventions in AD by affording clinicians insights into pathological degeneration of brain pathways (specifically memory) in AD.

Aims and Hypotheses

The aims of this study were twofold: first, to characterize MTL structures using surface-based procedures in A+ aMCI versus A+ AD dementia participants versus control participants, and, second, to relate shape features with episodic and procedural memory measures. It was ***hypothesized*** that A+ participants would exhibit more extensive surface-based abnormalities in hippocampal CA1 subfield regions and the entorhinal cortex relative to controls. It was also ***hypothesized*** that procedural and episodic memory performance would demonstrate unique relationships with distinct medial temporal regions – especially within the hippocampus – in A+ participants compared to healthy control participants.

Methods

Participant Recruitment

A total of 93 subjects (28 healthy control participants, “CON”; 48 aMCI participants, “aMCI”; 17 dementia participants, “AD”) were recruited through the West Virginia University School of Medicine memory health clinic between June 2020 and October 2023. Twenty-two of 93 initially included subjects were excluded from the study. Nine of these subjects experienced unresolved errors during data processing and were consequently excluded (2 CON, 5 aMCI, 2 AD). Additionally, 13 CON subjects were eliminated from the analysis to ensure statistical similarity in age between the CON-AD and CON-aMCI groups, resulting in N(AD)=16, N(aMCI) = 43, and N(CON)=13.

Participants’ amyloid positivity was determined using ^{18}F-Florbetaben Amyloid PET and/or CSF analysis of ABeta32 and p-tau/Beta42. All non-control subjects included in the current study were classified as amyloid positive (A+). T1-weighted 3T scans were obtained from each subject to confirm neurodegeneration.

Cognitive Measures

Each subject was administered a neuropsychological battery including a modified Trail-Making Test (TMT-M; Reitan & Wolfson, 2001), which measures procedural learning and memory retention, and the California Verbal Learning Test (CVLT; Delis et al., 2016), which measures verbal learning and memory retention. The initial diagnoses of aMCI or AD in all participants were determined based on the NIA-AA criteria by a multidisciplinary team comprising neurology, neuropsychology, neuroradiology, psychiatry, and geriatric attendings (McKhann et al., 2011).

MMSE

The Mini Mental State Exam (MMSE) is a cognitive assessment tool designed to screen for cognitive impairment and to estimate the severity and progression of cognitive deficits (Folstein et al., 1975). The MMSE evaluates functions including arithmetic, memory, and orientation through a series of questions and tasks. It is commonly used in clinical and research settings to assess cognitive function in individuals suspected of having dementia or related illnesses.

TMT-M

The Trail Making Test – Modified version (TMT-M) assesses procedural learning and retention. It is a version of the Trail Making Test (TMT) modified by researchers at West Virginia University. Specifically, participants completed Part A of the Trail Making Test (TMT-A), which involves connecting numbered dots randomly interspersed on a page in numerical order up to 25 (Reitan & Wolfson, 1985). This task measures psychomotor processing speed and visual-motor coordination. After an initial trial with standardized instructions, subsequent trials followed abbreviated instructions. The primary variable of interest was the time taken to complete each trial, with a maximum time score assigned if the subject exceeded the 150-second limit. Similar to other procedural learning tests, TMT-M involves learning skills with observable improvements after designated practice.

CVLT II

Episodic learning and retention were assessed using the CVLT-II Short Form (SF) following standard procedures outlined by Delis et al. (2000). Participants engaged in four learning trials, during which they were presented with a list of words. The primary

variable of interest was the number of words recalled across these learning trials. Standard learning and two-day delayed retention scores were obtained for both tasks. The learning slope calculation provided in the CVLT-II SF manual was not used. This approach allowed direct comparison between procedural and episodic learning, considering the total number of learning trials.

Procedural and episodic learning scores and retention percentages were calculated using the methodology outlined by Keith and colleagues (2022). Briefly, learning scores for the TMT-M and CVLT-II SF were calculated by taking the difference between first and last learning trials and standardizing the learning values, which adjusted for baseline performance and potential maximum gains. Retention scores were computed by determining the difference between initial and delayed trials, with procedural retention using the inverse of TMT-M time trial scores and episodic retention using CVLT scores, normalized to the baseline performance levels and scaled to a percentage.

Processing

T1-weighted images data from each subject were processed using the following pipelines: first, FreeSurfer (Dale et al., 1999), and second, the FreeSurfer-Initiated Large Deformation Diffeomorphic Metric Mapping pipeline (FS+LDDMM; Khan et al., 2008), which generates surface maps and segmentation of limbic and other subcortical structures – including the hippocampus – and, third, cortical parcellation for entorhinal cortex thickness.

FreeSurfer

The following explanation of FreeSurfer is standardized language from the FreeSurfer Wiki (*FreeSurfer Methods Citation - Free Surfer Wiki*, 2021), openly intended for this use. Cortical reconstruction and volumetric segmentation were performed with

the Freesurfer image analysis suite. The technical details of these procedures are described in

prior publications (Dale et al., 1999; Dale & Sereno, 1993; Fischl et al., 2001, 2002;). This processing includes motion correction and averaging (Reuter et al., 2010) of multiple volumetric T1 weighted images (when more than one is available), removal of non-brain tissue using a hybrid watershed/surface deformation procedure (Ségonne et al., 2004), automated Talairach transformation, segmentation of the subcortical white matter and deep gray matter volumetric structures (including hippocampus, amygdala, caudate, putamen, ventricles; Fischl et al., 2002;), intensity normalization (Sled et al., 1998), tessellation of the gray matter white matter boundary, automated topology correction (Fischl et al., 2001), and surface deformation following intensity gradients to optimally place the gray/white and gray/cerebrospinal fluid borders at the location where the greatest shift in intensity defines the transition to the other tissue class (Dale et al., 1999).

FSLDDMM

After initial FreeSurfer processing, surface features of the hippocampus were characterized using large deformation high dimensional brain mapping processes (Csernansky, Wang, et al., 2004). The specific method, large deformation diffeomorphic metric mapping (LDDMM), uses an atlas-based transformation that aligns a template representation of the hippocampus with each subject's voxel-derived hippocampus. Surfaces are then generated by overlaying a tessellated graph on each subject's image (A. R. Khan et al., 2008). The diffeomorphic transformation process allows individual surface points to be precisely matched to the template, preserving unique surface morphology of each structure. The resulting images of the hippocampus were then

manually inspected and corrected or reprocessed as necessary by trained raters to ensure the accuracy of each surface map.

Once all subjects were processed, the averaged surfaces of the hippocampus for each group (CON, aMCI, AD) were compared using a common template, resulting in data characterizing their degree of surface displacement. Hippocampal subfields of the CA1, subiculum, and combined CA2-4 and dentate gyrus (remainder) were then delineated on the surface for every subject using previously defined and validated borders from manual segmentations by a team of neuroanatomy experts who used reference sections based on the Duvernoy neuroanatomical atlas (Naidich et al., 2009). Group comparisons included CON-aMCI, CON-AD, and aMCI-AD.

Cortical Parcellation

Average entorhinal cortex thickness was also compared across groups. Parcellation of the entorhinal cortex followed the method by Desikan et al. (2006), a partially automated technique that differentiates cortical regions based on anatomical landmarks and gyral patterns. This approach combines manual tracing with automated algorithms applied to FS surfaces to ensure precise and replicable identification of the entorhinal cortex, and has been shown to be highly accurate (Desikan et al., 2006).

Analysis

Demographic data was analyzed using independent sample t-tests and chi-square analyses. Cognitive data was analyzed using analysis of variance (ANOVA) models, and cortical thickness differences between groups using applicable permutations of two-way analyses of covariance (ANCOVA) that control for short-term variability and relevant demographic and hemispheric distinctions. Hippocampal shape deformation between groups was analyzed using studentized t-tests for every vertex along the surface. Shape

deformation t-statistic contrast maps were created using all graphical vertices from the amalgamated surface. Random Field Theory (RFT) was used to correct for multiple comparisons in imaging (Worsley et al., 2004). RFT is used when a spatial component to the inferences exists, and reduces the chance of false positivity (Adler, 2010).

Bivariate Pearson correlation coefficients (for learning scores) and Spearman's rank correlation coefficient (for percent retention measurements) were calculated to evaluate relationships between cognitive performance and morphological metrics. The significance threshold was set to a p-value of 0.05. Post-hoc Tukey tests checked the significance between groups through multiple comparisons. Kruskal-Wallis tests assessed statistical significance of non-parametric data between groups (Keselman & Rogan, 1977; Kruskal & Wallis, 1952). Dunn's test was used to determine which pairs of groups had significantly different changes in episodic memory retention (Dunn, 1964). The Wilcoxon Rank Sum Test was used to compare entorhinal cortex thickness between pairs of groups (Wilcoxon, 1945). It is important to note that the methodology for this study only characterizes correlations between behavioral phenotypes and corresponding neural structure; therefore, any relationship discovered cannot claim causality.

Results

Demographics

Participant characteristics are displayed in Table 1. The sample was well-educated overall (M=15.67 years of education, *SD* = 3.55 years). Participants were majority white with three exceptions (all Asian). There were no significant differences between groups for age or education, but, as expected, there was a significant difference between groups in baseline MMSE scores, a marker of level of impairment (AD < aMCI < CON). No significant difference for sex was found between groups.

Table 1

Participant Demographics and Raw Cognitive Performance Scores

Variable	CON *n* = 12	aMCI *n* = 43	AD *n* = 16	*F* [a]	χ^2 [b]	*p*
Demographics						
Age	69 (7)	69 (7)	73 (6)	2.22		0.17
MMSE	30 (1)	27 (3)	25 (3)	**16.29**		<0.001
Education	15 (3)	16 (3)	16 (3)	0.39		0.68
Sex				3.903		0.14
Male	10 (63%)	3 (25%)	21 (49%)			
Female	6 (38%)	9 (75%)	22 (51%)			
Cognition						
CVLT Learning	20 (8)	12 (7)	8 (5)	**11.55**		<0.001
CVLT % Retention	96 (8)	52 (38)	24 (25)		**27.43**	<0.001
TMT Learning	14 (5)	10 (6)	8 (7)	**3.82**		0.03
TMT % Retention	94 (18)	91 (23)	102 (44)		0.19	0.91

Note. Standard deviations are in parentheses. MMSE =Mini Mental State Exam, CVLT = CVLT II – Short Form, TMT-M = modified Trail Making Test.

[a] One-way ANOVA. [b] Kruskal-Wallis test used for percentage-based measurements.

Cognitive performance

A main effect of episodic learning was found between groups ($F = 11.55$, $p < 0.001$; Table 1). Figure 1A illustrates a gradient of performance following diagnostic severity with healthy control participants scoring higher than aMCI and AD participants in episodic learning (CON > aMCI > AD). CON group episodic learning scores (mean = 19.72) differed with both aMCI (mean = 11.79; mean difference = 7.93, 95% CI [2.90, 12.96], $p < 0.001$) and AD (mean = 8.10; mean difference = 11.63, 95% CI [5.74, 17.51], $p < 0.001$) participant episodic learning scores. aMCI and AD episodic learning did not significantly differ from each other. Figure 1A additionally illustrates poorer performance in episodic memory retention in participants with aMCI and AD; indeed, a main effect was found between groups ($\chi^2 = 27.43$, $p < 0.001$; see Table 1).

Procedural memory learning trial analysis observed a main effect between groups, as illustrated in Figure 1B (F=3.82; p=0.03; see Table 1). However, significant differences were found only between CON (mean = 13.54) and AD groups (mean = 7.52; mean difference = 6.02, 95% CI [0.77, 11.27], p=0.02). No significant differences were detected between CON and aMCI (mean = 9.7) participants nor between aMCI and AD groups in procedural learning performance. Figure 1B shows that although procedural *learning* scores had a main effect between groups, there were no significant group differences to report in procedural memory *retention* scores ($\chi^2 = 0.19$, $p = 0.91$).

Upon later testing for retention ability, CON participants scored only 1 point worse on the episodic memory retention task than initial learning trials, an insignificant

Figure 1

Standardized Scores for Episodic and Procedural Memory Tests by Diagnostic Group

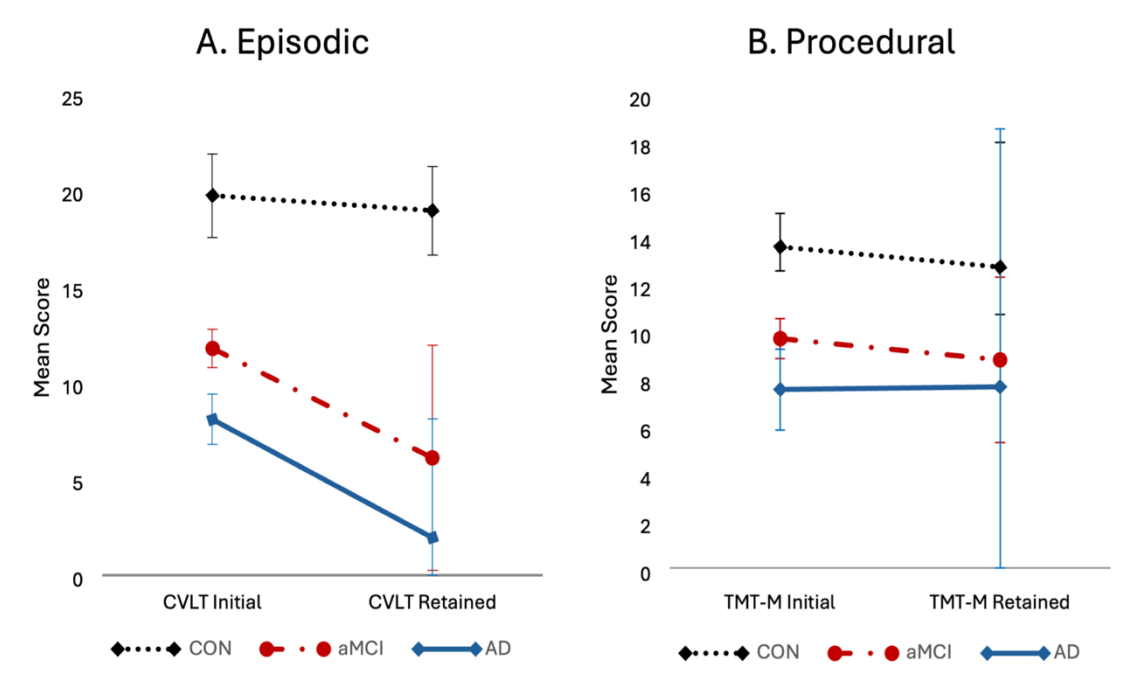

Note. "Initial" refers to performance score immediately after learning trials. "Retained" refers to later follow-up trial testing, measuring retention of knowledge or skill from the CVLT-II (Episodic) or TMT-M (Procedural) tests, respectively. (A) Comparison of episodic learning and retention across groups. (B) Comparison of procedural learning and retention across groups.

difference ($p > 0.05$). Notably, both aMCI (mean difference = 6.1) and AD (mean difference = 1.9) participants scored considerably lower than their respective initial learning trials ($\chi^2 = 20.88$, $p < 0.001$). Post-hoc Dunn tests revealed significant differences between the CON group and both the aMCI ($p = 0.003$) and AD ($p < 0.001$) groups. There was no significant difference between the aMCI and AD groups ($p = 0.07$). On the initial procedural learning tasks, CON participants (mean = 13.5) again scored nearly double AD participants (mean = 7.5), while aMCI participants (mean = 9.7) scored between CON and AD. However, later procedural learning retention trials showed a

moderate decrease in performance for CON (mean difference = 1.2) and aMCI (mean difference = 0.9) participants, while AD participants (mean difference = 0.1) showed a slight increase in performance. However, these differences were not statistically significant ($\chi^2 = 0.33$, $p = 0.85$). This pattern of results, with a significant decline in episodic but not procedural memory retention in aMCI and AD participants, is contrary to common expectations.

Figure 2A shows a decrease in episodic learning ability as the severity of patient diagnosis increases. Notably, episodic learning ability decreases at a steeper rate than procedural learning ability along the trajectory of symptom progression, eventually resulting in no difference for AD participants. This observation is supported by the

Figure 2

Learning Scores and Percent Retention on Episodic and Procedural Tests by Diagnostic Group

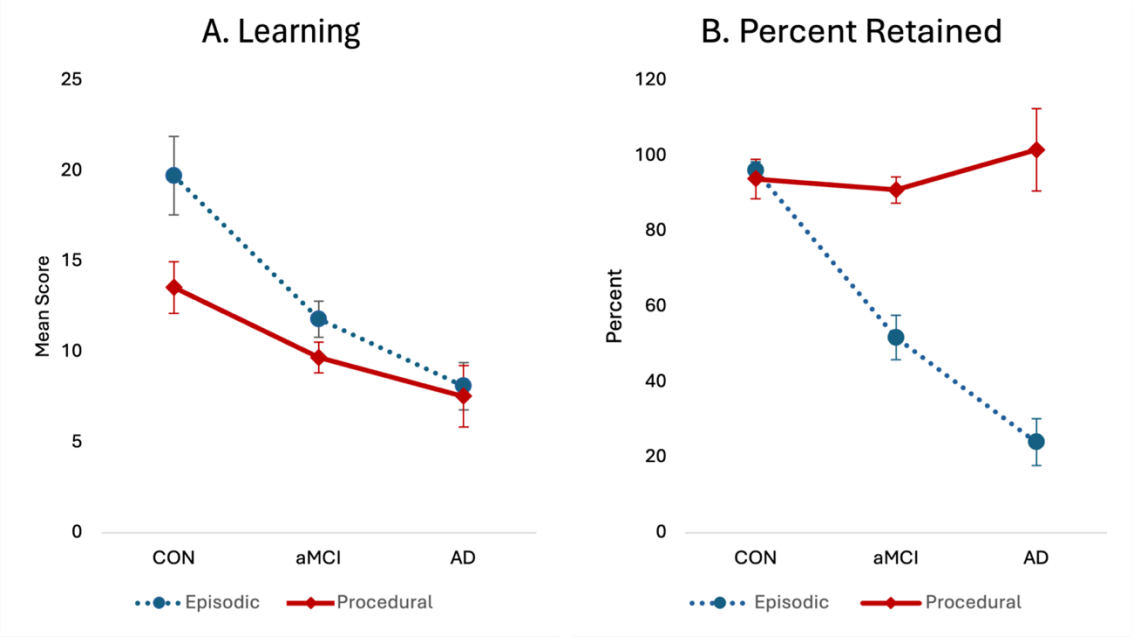

Note. Episodic scores are derived from CVLT-II performance. Procedural scores are derived from TMT-M performance. (A) Comparison of episodic and procedural learning across diagnostic groups. (B) Comparison of episodic and procedural memory retention across groups, expressed as a percentage of initial performance. Scores above 100% indicate

significant differences in episodic memory change scores between groups (χ^2= 20.88, p < 0.001), but not in procedural memory change scores (χ^2= 0.33, p = 0.85).

Figure 2B illustrates the percent retention of each group relative to initial performance on both episodic and procedural tests. CON participants retained episodic memory at the same rate as procedural memory, but aMCI participants retained episodic memory far worse than procedural memory (mean difference = 39.2%). AD participants not only retained all of procedural memory as tested, but actually improved in this measure (mean difference = 2.5%). This is in contrast with poor episodic memory retention rates (mean = 24%) for AD participants. The group differences in episodic memory retention were statistically significant (χ^2 = 20.88, p < 0.001), with significant post-hoc differences observed between the CON group and both the aMCI (p = 0.003) and AD (p < 0.001) groups. There was no significant difference between the aMCI and AD groups (p = 0.07). There were no significant differences between the groups in procedural memory retention (χ^2= 0.33, p = 0.85).

Surface-Based Analyses

Hippocampus

Hippocampal morphometric analysis revealed significant group findings, as shown in Figure 3. The most significant and widespread differences were observed in a contrast between CON-AD in the posterolateral portion of the CA1 region of the left

Figure 3

Hippocampal Shape Deformation Comparisons by Group

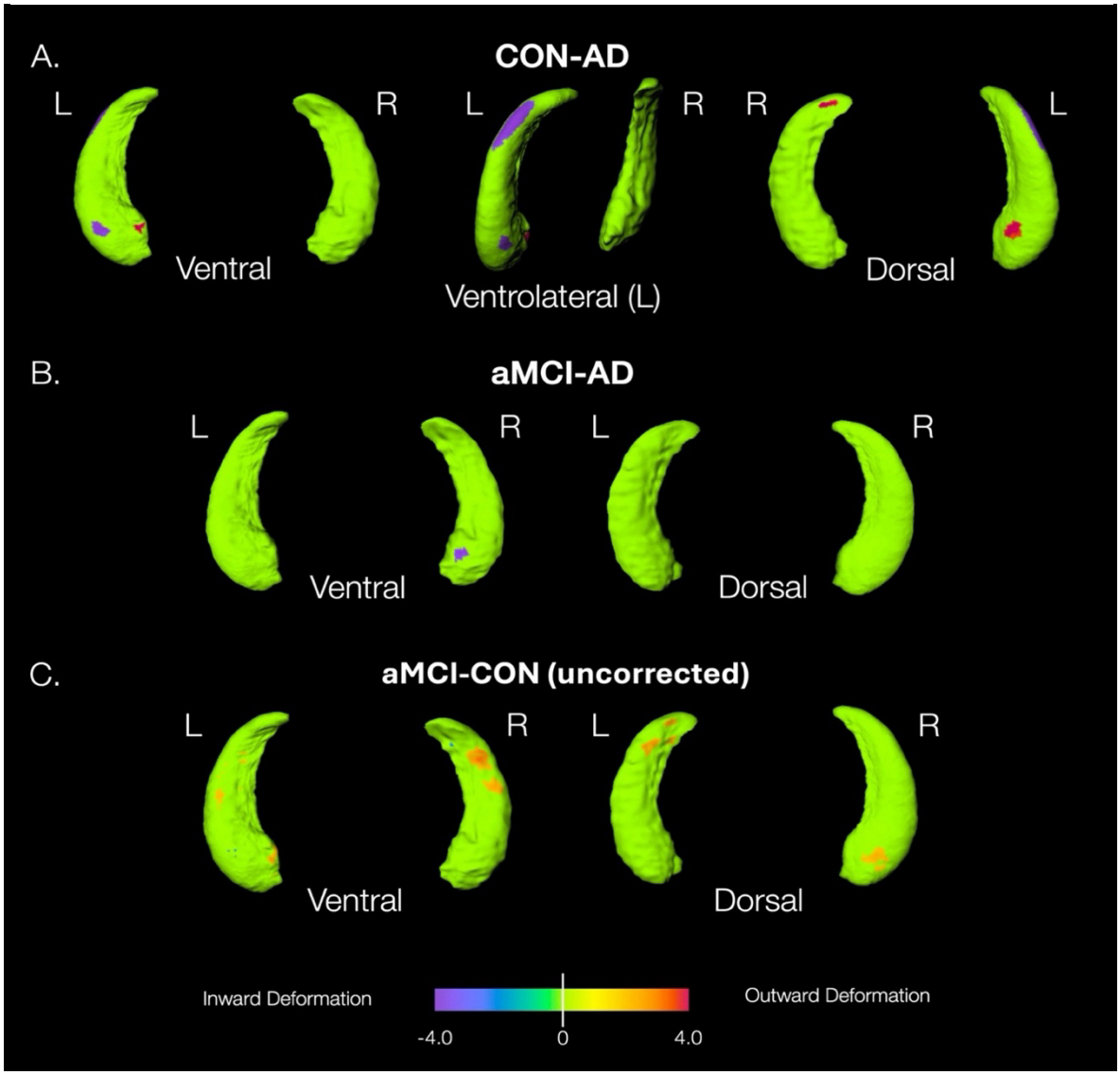

Note. Purple indicates inward deformation and red indicates outward deformation of the second group (e.g., AD) compared to the first (e.g., CON). Results are significant at $p < .05$, corrected for multiple comparisons using Random Field Theory (RFT), except in Panel C, which displays uncorrected results for exploratory purposes.

hippocampus, showing significant inward deformation (Figure 3A). Also present in the left hippocampus was anterior ventral CA1 inward deformation, and a slight extrusion in the anterior medial portion of the CA1 (Figure 3A). In the right hippocampus, the ventral portion of the subiculum also demonstrated significant outward deformation by the AD group versus healthy controls (Figure 3A). All aMCI-AD findings survived Random Field Theory correction.

Figure 3B illustrates the limited findings between aMCI and AD groups. Small inward deformation was detected on the border of the CA1 subfield and the subiculum, while no other findings survived Random Field Theory correction. Similarly, comparisons between aMCI and CON groups yielded no significant results (Figure 3C). Figure 3C shows uncorrected deformation values between aMCI and CON groups for exploratory purposes only. There are significant uncorrected findings bilaterally in both the subiculum and the CA1 regions.

Entorhinal Cortex

Table 2 shows entorhinal cortex thickness mean values and standard deviation. Raw entorhinal cortex mean thickness values followed the symptom progression of AD,

Table 2

Comparison of Entorhinal Cortex Thickness by Group

Group	Entorhinal Cortex Thickness					
	Left hemisphere		Right hemisphere		Average hemispheres	
	M	*SD*	*M*	*SD*	*M*	*SD*
AD	2.75	0.51	2.90	0.45	2.82	0.43
aMCI	2.92	0.38	3.14	0.34	3.03	0.33
CON	3.06	0.42	3.23	0.54	3.15	0.46

Note. For the purposes of this study, only averaged hemispheric measurements were used for later analyses.

with healthy control participants having the thickest entorhinal cortex on average (M = 1.95, SD = 0.22) and AD participants having the thinnest entorhinal cortex (M = 1.78, SD = 0.22) across both hemispheres individually and as an averaged hemispheric value.

One-way ANOVA revealed no significance between groups, but post-hoc analysis was required because of the nonparametric nature of the data; the Kruskal-Wallace test for non-parametric data revealed a significant main group effect of the averaged entorhinal cortex value (χ^2= 6.48, p=0.041). However, follow-up pairwise comparisons using the Wilcoxon Rank Sum test resulted in no group differences ($p > 0.05$).

Structure-Function Correlations

Pearson's correlation coefficients (mean score) and Spearman's rank correlations (percent retention) revealed several significant correlations with both hippocampal regions and entorhinal cortex thickness, as shown in Table 3. Correlations reported are those calculated from the bilateral deformation averages of the hippocampal regions CA1, subiculum, remaining hippocampal regions (remainder), bilateral thickness averages of the entorhinal cortex, and cognitive performance as measured by CVLT-II (episodic) learning and retention and TMT-M (procedural) learning and retention. Correlations by hemisphere were also calculated, but because hemispheric correlations were not included in the study design the results are found in the Appendix Table S1.

In AD participants, there was a strong positive correlation (0.67) between episodic retention and the CA1 region of the hippocampus ($p = 0.005$). A moderate negative correlation in AD (-0.51) was observed in hippocampal regions not associated with

Table 3

Brain Region and Memory Performance Correlations by Group

Group	Structure	Episodic Learning		Episodic % Retention		Procedural Learning		Procedural % Retention	
		r [a]	p	r_s [b]	p	r [a]	p	r_s [b]	p
CON									
	CA1	0.16	0.62	-0.37	0.24	0.12	0.72	0.14	0.67
	Subiculum	-0.37	0.24	0.31	0.33	-0.18	0.58	0.31	0.33
	Remainder	-0.31	0.33	0.20	0.53	-0.11	0.74	0.15	0.65
	Entorhinal	-0.18	0.57	0.44	0.15	-0.08	0.80	-0.33	0.30
aMCI									
	CA1	**0.42**	0.005	**0.36**	0.017	0.10	0.51	**-0.35**	0.022
	Subiculum	0.28	0.06	0.20	0.19	0.28	0.07	-0.25	0.10
	Remainder	-0.22	0.16	-0.19	0.22	0.26	0.10	-0.04	0.81
	Entorhinal	-0.04	0.82	0.11	0.50	0.08	0.60	0.00	0.99
AD									
	CA1	0.34	0.19	**0.67**	0.005	0.20	0.46	-0.23	0.39
	Subiculum	-0.03	0.90	0.00	0.99	0.13	0.62	-0.06	0.83
	Remainder	**-0.51**	0.043	-0.26	0.34	-0.17	0.54	0.02	0.95
	Entorhinal	**0.51**	0.042	0.39	0.13	**0.57**	0.022	-0.40	0.13

Note. Episodic scores are derived from CVLT-II performance. Procedural scores are derived from TMT-M performance.

[a] r = Pearson Correlation Coefficient. [b] r_s = Spearman Rank Correlations; used for percentage-based correlations.

neither the subiculum nor the CA1 region (p = 0.04). The entorhinal cortex was moderately associated with both episodic (0.51; p = 0.04) and procedural (0.57; p = 0.02) learning measures in AD participants.

The CA1 region was frequently correlated with cognitive measures in aMCI participants. There was a moderate positive correlation with both episodic learning (0.42, p = 0.005) and episodic retention (0.36; p = 0.02). Additionally, a moderate negative correlation (-0.35) with procedural retention (p = 0.02) was discovered, a correlation that

is notable for appearing only in the aMCI group and not the AD group. No other regions were significantly associated with cognitive performance in aMCI participants. Additionally, no correlations were found between brain region integrity and cognitive measures in healthy control participants.

Discussion and Analysis

The current study compared episodic learning and retention with procedural learning and retention, and characterized hippocampal shape and entorhinal thickness, correlating surface-based measurements with episodic and procedural learning and retention in amyloid-positive (A+) participants with diagnoses of amnestic mild cognitive impairment (aMCI) and dementia of the Alzheimer's type (AD). It was primarily hypothesized that A+ participants would exhibit more severe surface-based abnormalities in the hippocampal CA1 region and the entorhinal cortex relative to controls. The findings were partially consistent with the hypothesis as A+ participants (specifically AD dementia participants) were shown to have greater inward deformation in the CA1 region of the hippocampus relative to both control and aMCI participants. There were also main effects for group differences in the entorhinal cortex as clarified; however, no significant differences were detected between A+ aMCI participants and healthy control participants after correcting for multiple comparisons.

It was also hypothesized that A+ participants would demonstrate unique correlations of procedural and episodic memory performance within the hippocampus. Calculations of Pearson's correlation coefficients and Spearman's rank correlations provided evidence in support of this hypothesis, finding there to be several significant correlations between hippocampal subregions and cognitive measures in the A+ participant groups (AD and aMCI), but not in healthy control participants. Specifically, in AD participants, there was a strong positive correlation between episodic retention and the CA1 region of the hippocampus, and moderate correlations between the entorhinal cortex and both episodic and procedural learning measures. In aMCI participants, the

CA1 region showed moderate positive correlations with both episodic learning and retention, while also exhibiting a moderate negative correlation with procedural retention.

It is important to note the progressive nature of AD pathology when discussing neurologic deformation. AD has been shown to be a result of premature neuronal death, with cognitive symptoms appearing after significant damage has been done to target brain regions. The current study focused on the early stage of the disease (amnestic Mild Cognitive Impairment; aMCI) compared to the advanced stage of the disease (dementia of the Alzheimer's type; AD). Examining the differences between these two groups, as well as the differences between healthy control participants and aMCI participants, can result in greater understanding of the pathological progression of the disease, thereby informing the focus of future studies. This morphological study examined the pathological progression in terms of hippocampal shape, entorhinal cortex thickness, and correlations between those anatomical and cognitive measures.

Previous studies have identified the hippocampus as a severely affected target of neurodegeneration in participants with cognitive and biological markers for AD (Chauveau et al., 2021; Csernansky, Hamstra, et al., 2004). Limitations with volumetric methodology restricted most studies to date to investigate only hippocampal volume, including subfield volume such as CA1 and the subiculum, in relation to AD biomarkers such as beta amyloid plaques (Jack et al., 1999; Wisse et al., 2014). Follow-up studies have sought to corroborate those findings with added specificity using morphologic methods such as those used in the current study; recent findings corroborate the initial findings of hippocampal atrophy in the CA1 subregion, albeit with greater specificity. For example, Busatto Filho et al., (2021) found there to be inward deformation in the anterior

and especially the posterior portion of the hippocampal CA1 subfield in AD-confirmed participants compared to healthy controls.

The current study corroborated those findings, with a left-lateralized discovery of posterior CA1 inward deformation in AD. Curiously, Busatto Filho and colleagues (2021) found no correlation with amyloid plaque presence and neurodegeneration; however, the current study of amyloid-positive participants showed atrophy in the posterior CA1 subfield in AD dementia participants, and in the anterior CA1 in A+ participants. Though no specific correlations were calculated with amyloid-positivity, this study's findings of CA1 deformation in participants with AD contributes to the growing field of literature concerning the amyloid-beta hypothesis of AD (Selkoe & Hardy, 2016).

Additionally, the unilateral nature of the inward deformation in AD is significant, as it has been shown that the left hippocampal formation is more significantly linked to memory than is the right hippocampus (Das et al., 2009). A study by Zhu et al. (2023) found that both the volume and shape of the left and right hippocampus changed distinctly and rapidly after AD diagnosis, with the left hemisphere exhibiting greater atrophy; the current study endorses this finding. Additionally, the foci of CA1 deformation as illustrated in Figure 3A could suggest the existence of more specific subfield delineation as the correlation between function and structure becomes better defined.

AD participants showed the most significant atrophy in the posterior CA1 subfield, while aMCI participants also displayed some atrophy in the anterior CA1 subfield as compared to AD participants. While no significant differences survived between control participants and aMCI subjects, the CON-AD comparison garnered real

and clinically important information about the progression of AD pathology: it appears that AD progression most severely targets the posterior portion of the CA1 region, though, using the aMCI group results as a temporal checkpoint, the apparent rate of atrophy may be highest in the anterior portion of the CA1 subregion in participants with amyloid positivity. Development of accurate characterization of hippocampal degenerative pathophysiology using morphological methodology may serve as a helpful imaging marker to monitor clinical AD progression.

Though small, a main group effect was found for the entorhinal cortex across all groups, although this finding disappeared upon submission to pairwise comparisons. This was an unexpected finding, given the extensive literature showing entorhinal atrophy as the chronological first target of AD pathology (Du et al., 2004; U. A. Khan et al., 2014). The small sample size of the study (N=93; CON n=12, aMCI n=43, AD n=16), undoubtedly limited the ability to detect smaller effect sizes for entorhinal cortex thickness between groups.

The correlation analyses revealed several important relationships between regional brain morphometry and cognitive performance in the amyloid-positive participant groups. In AD dementia participants, episodic memory retention as measured by the CVLT was strongly and positively correlated with the integrity of the CA1 subfield of the hippocampus. This aligns with the well-established role of the CA1 in memory consolidation and its vulnerability to neuropathological changes in Alzheimer's disease. Interestingly, entorhinal cortical thickness also showed moderate positive correlations with both episodic and procedural learning abilities in AD. As the entorhinal cortex

provides the major input and output pathways of the hippocampus, its structural integrity likely affects both memory systems (Reagh & Yassa, 2014).

In aMCI participants, a pattern of correlations emerged that may capture earlier disease processes. Similar to the AD group, the aMCI group's CA1 subfield showed moderate positive correlations with episodic learning and retention, reinforcing its proven and central role in episodic memory performance (Mueller et al., 2010). A unique moderate negative correlation was found between CA1 morphology and procedural memory retention in aMCI, which was not observed in either healthy control participants or AD dementia. This unexpected finding may reflect the CA1 subfield's involvement in procedural memory in healthy systems, an involvement which is gradually ceded to compensatory mechanisms as the brain continues to atrophy. Beaunieux et al. (2012) provided initial evidence for this conjecture, showing that as performance decreased in episodic memory systems, procedural memory performance was maintained despite brain-wide atrophy.

Indeed, the current study found that while AD participants performed worse than control participants and aMCI participants on initial procedural memory tests, they uniquely demonstrated improved retention of procedural memories compared to their initial learning scores. This pattern contrasts starkly with their impaired episodic memory retention and corroborates work done by Keith et al. (2023). As proposed by Beaunieux et al. (2012) and mentioned above, one possible explanation is that neural resources normally assigned to episodic memory systems – such as the hippocampus, which degenerates early in AD – may be reallocated to help support procedural memory systems that are relatively spared. It is also possible that the observed improvement in procedural

retention could be attributable to other factors. For instance, memory consolidation may have occurred during REM sleep, which is known to enhance procedural skill learning (Plihal & Born, 1997; Tucker et al., 2006). Additionally, poor procedural baseline task performance in AD may have created a floor effect where any minor fluctuations in performance were amplified as seeming gains in retention scores. Together these results suggest a unique process of potential neural compensation in the progression of AD pathology that warrants further investigation. No significant brain-cognition correlations were detected in healthy control participants, suggesting these relationships may be specific to underlying Alzheimer's pathology.

The current study's focus on amyloid-positive (A+) participants across the Alzheimer's spectrum produced novel insights into how brain morphology could be affected by amyloid pathology. Hippocampal subfields and the entorhinal cortex both had significant correlations with different memory measures in AD and aMCI groups that were distinct from healthy control participants, suggesting a close association with structure-function relationships in memory circuits. This study provided a characterization of the specific hippocampal morphology of A+ participants, and provided a glimpse into the morphological progression of AD. Longitudinal studies utilizing morphological methodology to track shape changes in relation to amyloid accumulation over time could clarify whether these alterations are the consequences or causes of neural amyloidosis.

This study has several limitations that are important to acknowledge. Primarily, the sample size was modest, limiting the power of the study. Ideally, each group would have at least 50-100 participants to improve morphologic sensitivity and reduce the

probability of both Type I and Type II errors. Larger data sets provide a better representation of trends in pathology, and neuropathology is no different. Groups like the Alzheimer's Disease Neuroimaging Initiative (ADNI; Petersen et al., 2010) are improving access to data to be used for meta-analysis; future studies should utilize this resource and similar to improve morphological sensitivity to disease. The diversity of participants was low, as the sample was largely well educated and almost entirely white, reducing the study's generalizability. Additionally, the TMT-M test used to measure procedural learning has not been independently validated yet as a measure of procedural learning and retention, though the developers continue to work towards that end (Keith et al., 2023). Despite these limitations, appropriate statistical analyses resulted in medium to large correlations largely supporting the hypotheses.

Beyond the limitations, the study has several strengths that should be emphasized. First of all, each participant was diagnosed with AD or aMCI clinically first, then confirmed to have amyloid positivity through either ^{18}F-Florbetaben Amyloid PET and/or CSF analysis of ABeta32 and p-tau/Beta42. Such affirmative diagnosis is a luxury that bestows high confidence in the results of the study as they refer to diagnostic relatability. Second, morphologic methodology is highly sensitive and reliable, providing assurance in the precision of its results. Correlating morphologic and cortical thickness data with cognitive measures allowed us to explore the underlying anatomical structures for each task. Third, we compared procedural and episodic memory in participants with both aMCI and AD dementia, a largely unexplored topic.

Future studies should focus on expanding the scope of this project by replicating with larger data sets and expanding the structures of focus. Importantly, other subcortical

structures such as the basal ganglia are highly associated with motor function, a main component of procedural memory. Investigating these subcortical features in relation to memory systems could elucidate novel relationships that were impossible to characterize using volumetric analysis. Future work could also be devoted to identifying interactions between episodic and procedural memory systems through correlative and interactive analyses.

Conclusion

In summary, this study utilized advanced surface- and thickness-based morphometric analyses to characterize regionally specific changes in the hippocampus and the entorhinal cortex in amyloid-positive (A+) participants on the Alzheimer's disease continuum. Posterior CA1 hippocampal subfield deformations were detected in A+ Alzheimer's dementia (AD) participants relative to controls and amnestic MCI (aMCI) participants, suggesting that CA1 atrophy is a potential hallmark of AD progression. Correlations between these morphometric measures in AD participants and procedural and episodic memory measures revealed strong positive correlations between the integrity of the CA1 subfield of the hippocampus and episodic memory retention, as well as moderate correlations between entorhinal cortex thickness and both episodic and procedural learning abilities. In aMCI participants, the CA1 subfield showed moderate positive associations with episodic learning and retention, along with a unique moderate negative correlation with procedural memory retention that was not present in controls or AD participants. This pattern may reflect a compensatory mechanism in the early stages of AD, where procedural memory is preserved as episodic memory declines. These findings highlight how morphological techniques can illuminate highly specific brain-behavior relationships that could not be captured by volumetric analysis alone, offering new insights into the complex interplay between brain structure and cognitive function in AD and potentially informing the development of novel diagnostic and therapeutic approaches.

References

2023 Alzheimer's disease facts and figures. (2023). *Alzheimer's & Dementia*, *19*(4), 1598–1695. https://doi.org/10.1002/alz.13016

Adler, R. J. (2010). *The Geometry of Random Fields* (SIAM ed). Society for Industrial and Applied Mathematics.

Beaunieux, H., Eustache, F., Busson, P., de la Sayette, V., Viader, F., & Desgranges, B. (2012). Cognitive procedural learning in early Alzheimer's disease: Impaired processes and compensatory mechanisms. *Journal of Neuropsychology*, *6*(1), 31–42. https://doi.org/10.1111/j.1748-6653.2011.02002.x

Bracko, O., Cruz Hernández, J. C., Park, L., Nishimura, N., & Schaffer, C. B. (2021). Causes and consequences of baseline cerebral blood flow reductions in Alzheimer's disease. *Journal of Cerebral Blood Flow & Metabolism*, *41*(7), 1501–1516. https://doi.org/10.1177/0271678X20982383

Busatto Filho, G., Duran, F. L. de S., Squarzoni, P., Coutinho, A. M. N., Rosa, P. G. P., Torralbo, L., Pachi, C. G. da F., da Costa, N. A., Porto, F. H. de G., Carvalho, C. L., Brucki, S. M. D., Nitrini, R., Forlenza, O. V., Leite, C. da C., Buchpiguel, C. A., & de Paula Faria, D. (2021). Hippocampal subregional volume changes in elders classified using positron emission tomography-based Alzheimer's biomarkers of β-amyloid deposition and neurodegeneration. *Journal of Neuroscience Research*, *99*(2), 481–501. https://doi.org/10.1002/jnr.24739

Chauveau, L., Kuhn, E., Palix, C., Felisatti, F., Ourry, V., de La Sayette, V., Chételat, G., & de Flores, R. (2021). Medial temporal lobe subregional atrophy in aging and

Alzheimer's disease: A longitudinal study. *Frontiers in Aging Neuroscience*, *13*, 750154. https://doi.org/10.3389/fnagi.2021.750154

Csernansky, J. G., Hamstra, J., Wang, L., McKeel, D., Price, J. L., Gado, M., & Morris, J. C. (2004). Correlations between antemortem hippocampal volume and postmortem neuropathology in AD subjects. *Alzheimer Disease & Associated Disorders*, *18*(4), 190.

Csernansky, J. G., Wang, L., Joshi, S. C., Ratnanather, J. T., & Miller, M. I. (2004). Computational anatomy and neuropsychiatric disease: Probabilistic assessment of variation and statistical inference of group difference, hemispheric asymmetry, and time-dependent change. *NeuroImage*, *23 Suppl 1*, S56-68. https://doi.org/10.1016/j.neuroimage.2004.07.025

Dale, A. M., Fischl, B., & Sereno, M. I. (1999). Cortical surface-based analysis: I. segmentation and surface reconstruction. *NeuroImage*, *9*(2), 179–194. https://doi.org/10.1006/nimg.1998.0395

Dale, A. M., & Sereno, M. I. (1993). Improved localizadon of cortical activity by combining EEG and MEG with MRI cortical surface reconstruction: A linear approach. *Journal of Cognitive Neuroscience*, *5*(2), 162–176. https://doi.org/10.1162/jocn.1993.5.2.162

Das, S. R., Mechanic-Hamilton, D., Korczykowski, M., Pluta, J., Glynn, S., Avants, B. B., Detre, J. A., & Yushkevich, P. A. (2009). Structure specific analysis of the hippocampus in temporal lobe epilepsy. *Hippocampus*, *19*(6), 517–525. https://doi.org/10.1002/hipo.20620

Delis, D. C., Kramer, J. H., Kaplan, E., & Ober, B. A. (2016). *California Verbal Learning Test—Second Edition* [dataset]. https://doi.org/10.1037/t15072-000

Desikan, R. S., Ségonne, F., Fischl, B., Quinn, B. T., Dickerson, B. C., Blacker, D., Buckner, R. L., Dale, A. M., Maguire, R. P., Hyman, B. T., Albert, M. S., & Killiany, R. J. (2006). An automated labeling system for subdividing the human cerebral cortex on MRI scans into gyral based regions of interest. *NeuroImage*, *31*(3), 968–980. https://doi.org/10.1016/j.neuroimage.2006.01.021

Du, A. T., Schuff, N., Kramer, J. H., Ganzer, S., Zhu, X. P., Jagust, W. J., Miller, B. L., Reed, B. R., Mungas, D., Yaffe, K., Chui, H. C., & Weiner, M. W. (2004). Higher atrophy rate of entorhinal cortex than hippocampus in AD. *Neurology*, *62*(3), 422–427.

Dunn, O. J. (1964). Multiple comparisons using rank sums. *Technometrics*, *6*(3), 241–252. https://doi.org/10.1080/00401706.1964.10490181

Eichenbaum, H., & Lipton, P. A. (2008). Towards a functional organization of the medial temporal lobe memory system: Role of the parahippocampal and medial entorhinal cortical areas. *Hippocampus*, *18*(12), 1314–1324. https://doi.org/10.1002/hipo.20500

Ferretti, M. T., Iulita, M. F., Cavedo, E., Chiesa, P. A., Schumacher Dimech, A., Santuccione Chadha, A., Baracchi, F., Girouard, H., Misoch, S., Giacobini, E., Depypere, H., & Hampel, H. (2018). Sex differences in Alzheimer disease—The gateway to precision medicine. *Nature Reviews Neurology*, *14*(8), 457–469. https://doi.org/10.1038/s41582-018-0032-9

Fischl, B., & Dale, A. M. (2000). Measuring the thickness of the human cerebral cortex from magnetic resonance images. *Proceedings of the National Academy of Sciences of the United States of America*, *97*(20), 11050–11055. https://doi.org/10.1073/pnas.200033797

Fischl, B., Liu, A., & Dale, A. M. (2001). Automated manifold surgery: Constructing geometrically accurate and topologically correct models of the human cerebral cortex. *IEEE Transactions on Medical Imaging*, *20*(1), 70–80. https://doi.org/10.1109/42.906426

Fischl, B., Salat, D. H., Busa, E., Albert, M., Dieterich, M., Haselgrove, C., van der Kouwe, A., Killiany, R., Kennedy, D., Klaveness, S., Montillo, A., Makris, N., Rosen, B., & Dale, A. M. (2002). Whole brain segmentation: Automated labeling of neuroanatomical structures in the human brain. *Neuron*, *33*(3), 341–355. https://doi.org/10.1016/s0896-6273(02)00569-x

Fischl, B., Salat, D. H., van der Kouwe, A. J. W., Makris, N., Ségonne, F., Quinn, B. T., & Dale, A. M. (2004). Sequence-independent segmentation of magnetic resonance images. *NeuroImage*, *23 Suppl 1*, S69-84. https://doi.org/10.1016/j.neuroimage.2004.07.016

Fischl, B., Sereno, M. I., & Dale, A. M. (1999). Cortical surface-based analysis. II: Inflation, flattening, and a surface-based coordinate system. *NeuroImage*, *9*(2), 195–207. https://doi.org/10.1006/nimg.1998.0396

Fischl, B., Sereno, M. I., Tootell, R. B. H., & Dale, A. M. (1999). High-resolution intersubject averaging and a coordinate system for the cortical surface. *Human*

Brain Mapping, *8*(4), 272–284. https://doi.org/10.1002/(SICI)1097-0193(1999)8:4<272::AID-HBM10>3.0.CO;2-4

Fischl, B., van der Kouwe, A., Destrieux, C., Halgren, E., Ségonne, F., Salat, D. H., Busa, E., Seidman, L. J., Goldstein, J., Kennedy, D., Caviness, V., Makris, N., Rosen, B., & Dale, A. M. (2004). Automatically parcellating the human cerebral cortex. *Cerebral Cortex*, *14*(1), 11–22. https://doi.org/10.1093/cercor/bhg087

Folstein, M. F., Folstein, S. E., & McHugh, P. R. (1975). "Mini-mental state": A practical method for grading the cognitive state of patients for the clinician. *Journal of Psychiatric Research*, *12*(3), 189–198. https://doi.org/10.1016/0022-3956(75)90026-6

FreeSurfer Methods Citation—Free Surfer Wiki. (2021). https://surfer.nmr.mgh.harvard.edu/fswiki/FreeSurferMethodsCitation

Giacobini, E., & Gold, G. (2013). Alzheimer disease therapy—Moving from amyloid-β to tau. *Nature Reviews Neurology*, *9*(12), Article 12. https://doi.org/10.1038/nrneurol.2013.223

Goyal, M. S., Blazey, T., Metcalf, N. V., McAvoy, M. P., Strain, J. F., Rahmani, M., Durbin, T. J., Xiong, C., Benzinger, T. L.-S., Morris, J. C., Raichle, M. E., & Vlassenko, A. G. (2023). Brain aerobic glycolysis and resilience in Alzheimer disease. *Proceedings of the National Academy of Sciences of the United States of America*, *120*(7), e2212256120. https://doi.org/10.1073/pnas.2212256120

Han, X., Jovicich, J., Salat, D., van der Kouwe, A., Quinn, B., Czanner, S., Busa, E., Pacheco, J., Albert, M., Killiany, R., Maguire, P., Rosas, D., Makris, N., Dale, A., Dickerson, B., & Fischl, B. (2006). Reliability of MRI-derived measurements of

human cerebral cortical thickness: The effects of field strength, scanner upgrade and manufacturer. *NeuroImage*, *32*(1), 180–194. https://doi.org/10.1016/j.neuroimage.2006.02.051

Hardy, J. A., & Higgins, G. A. (1992). Alzheimer's disease: The amyloid cascade hypothesis. *Science*, *256*(5054).

Honig, L. S., Kang, M. S., Lee, A. J., Reyes-Dumeyer, D., Piriz, A., Soriano, B., Franco, Y., Coronado, Z. D., Recio, P., Mejía, D. R., Medrano, M., Lantigua, R. A., Teich, A. F., Dage, J. L., & Mayeux, R. (2023). Evaluation of plasmabiomarkers for A/T/N classification of Alzheimer disease among adults of Caribbean Hispanic ethnicity. *JAMA Network Open*, *6*(4), e238214. https://doi.org/10.1001/jamanetworkopen.2023.8214

Jack, C. R., Bennett, D. A., Blennow, K., Carrillo, M. C., Dunn, B., Haeberlein, S. B., Holtzman, D. M., Jagust, W., Jessen, F., Karlawish, J., Liu, E., Molinuevo, J. L., Montine, T., Phelps, C., Rankin, K. P., Rowe, C. C., Scheltens, P., Siemers, E., Snyder, H. M., … Contributors. (2018). NIA-AA research framework: Toward a biological definition of Alzheimer's disease. *Alzheimer's & Dementia: The Journal of the Alzheimer's Association*, *14*(4), 535–562. https://doi.org/10.1016/j.jalz.2018.02.018

Jack, C. R., Petersen, R. C., Xu, Y. C., O'Brien, P. C., Smith, G. E., Ivnik, R. J., Boeve, B. F., Waring, S. C., Tangalos, E. G., & Kokmen, E. (1999). Prediction of AD with MRI-based hippocampal volume in mild cognitive impairment. *Neurology*, *52*(7), 1397–1403.

Jack, C. R., Wiste, H. J., Weigand, S. D., Therneau, T. M., Knopman, D. S., Lowe, V., Vemuri, P., Mielke, M. M., Roberts, R. O., Machulda, M. M., Senjem, M. L., Gunter, J. L., Rocca, W. A., & Petersen, R. C. (2017). Age-specific and sex-specific prevalence of cerebral β-amyloidosis, tauopathy, and neurodegeneration in cognitively unimpaired individuals aged 50–95 years: A cross-sectional study. *The Lancet Neurology*, *16*(6), 435–444. https://doi.org/10.1016/S1474-4422(17)30077-7

Jahn, H. (2013). Memory loss in Alzheimer's disease. *Dialogues in Clinical Neuroscience*, *15*(4), 445–454. https://doi.org/10.31887/DCNS.2013.15.4/hjahn

Jovicich, J., Czanner, S., Greve, D., Haley, E., van der Kouwe, A., Gollub, R., Kennedy, D., Schmitt, F., Brown, G., MacFall, J., Fischl, B., & Dale, A. (2006). Reliability in multi-site structural MRI studies: Effects of gradient non-linearity correction on phantom and human data. *NeuroImage*, *30*(2), 436–443. https://doi.org/10.1016/j.neuroimage.2005.09.046

Keith, C. M., McCuddy, W. T., Lindberg, K., Miller, L. E., Bryant, K., Mehta, R. I., Wilhelmsen, K., Miller, M., Navia, R. O., Ward, M., Deib, G., D'Haese, P.-F., & Haut, M. W. (2023). Procedural learning and retention relative to explicit learning and retention in mild cognitive impairment and Alzheimer's disease using a modification of the trail making test. *Aging, Neuropsychology, and Cognition*, *30*(5), 669–686. https://doi.org/10.1080/13825585.2022.2077297

Keselman, H. J., & Rogan, J. C. (1977). The Tukey Multiple Comparison Test: 1953-1976. *Psychological Bulletin*, *84*(5), 1050–1056.

Khan, A. R., Wang, L., & Beg, M. F. (2008). FreeSurfer-initiated fully-automated subcortical brain segmentation in MRI using Large Deformation Diffeomorphic Metric Mapping. *NeuroImage*, *41*(3), 735–746. https://doi.org/10.1016/j.neuroimage.2008.03.024

Khan, U. A., Liu, L., Provenzano, F. A., Berman, D. E., Profaci, C. P., Sloan, R., Mayeux, R., Duff, K. E., & Small, S. A. (2014). Molecular drivers and cortical spread of lateral entorhinal cortex dysfunction in preclinical Alzheimer's disease. *Nature Neuroscience*, *17*(2), 304–311. https://doi.org/10.1038/nn.3606

Kropotov, J. D. (2009). Memory systems. In *Quantitative EEG, Event-Related Potentials and Neurotherapy* (pp. 310–324). Elsevier. https://doi.org/10.1016/B978-0-12-374512-5.00014-1

Kruskal, W. H., & Wallis, W. A. (1952). Use of ranks in one-criterion variance analysis. *Journal of the American Statistical Association*, *47*(260), 583–621. https://doi.org/10.1080/01621459.1952.10483441

Long, S., Benoist, C., & Weidner, W. (2023). *World Alzheimer Report 2023: Reducing dementia risk: Never too early, never too late*. Alzheimer's Disease International. https://www.alzint.org/resource/world-alzheimer-report-2023/

McKhann, G. M., Knopman, D. S., Chertkow, H., Hyman, B. T., Jack Jr., C. R., Kawas, C. H., Klunk, W. E., Koroshetz, W. J., Manly, J. J., Mayeux, R., Mohs, R. C., Morris, J. C., Rossor, M. N., Scheltens, P., Carrillo, M. C., Thies, B., Weintraub, S., & Phelps, C. H. (2011). The diagnosis of dementia due to Alzheimer's disease: Recommendations from the National Institute on Aging-Alzheimer's Association

workgroups on diagnostic guidelines for Alzheimer's disease. *Alzheimer's & Dementia*, *7*(3), 263–269. https://doi.org/10.1016/j.jalz.2011.03.005

Mueller, S. G., Schuff, N., Yaffe, K., Madison, C., Miller, B., & Weiner, M. W. (2010). Hippocampal atrophy patterns in mild cognitive impairment and Alzheimer's disease. *Human Brain Mapping*, *31*(9), 1339–1347. https://doi.org/10.1002/hbm.20934

Naidich, T. P., Haacke, E. M., Kollias, S. S., Sorensen, A. G., Duvernoy, H. M., & Delman, B. N. (2009). *Duvernoy's Atlas of the Human Brain Stem and Cerebellum: High-Field MRI: Surface Anatomy, Internal Structure, Vascularization and 3D Sectional Anatomy*. Springer Vienna Springer e-books.

Núñez, C., Callén, A., Lombardini, F., Compta, Y., Stephan-Otto, C., & for the Alzheimer's Disease Neuroimaging Initiative. (2020). Different cortical gyrification patterns in Alzheimer's disease and Impact on memory performance. *Annals of Neurology*, *88*(1), 67–80. https://doi.org/10.1002/ana.25741

Oveisgharan, S., Arvanitakis, Z., Yu, L., Farfel, J., Schneider, J. A., & Bennett, D. A. (2018). Sex differences in Alzheimer's disease and common neuropathologies of aging. *Acta Neuropathologica*, *136*(6), 887–900. https://doi.org/10.1007/s00401-018-1920-1

Parnetti, L., Chipi, E., Salvadori, N., D'Andrea, K., & Eusebi, P. (2019). Prevalence and risk of progression of preclinical Alzheimer's disease stages: A systematic review and meta-analysis. *Alzheimer's Research & Therapy*, *11*(1), 7. https://doi.org/10.1186/s13195-018-0459-7

Petersen, R. C., Aisen, P. S., Beckett, L. A., Donohue, M. C., Gamst, A. C., Harvey, D. J., Jack, C. R., Jagust, W. J., Shaw, L. M., Toga, A. W., Trojanowski, J. Q., & Weiner, M. W. (2010). Alzheimer's Disease Neuroimaging Initiative (ADNI): Clinical characterization. *Neurology*, *74*(3), 201–209. https://doi.org/10.1212/WNL.0b013e3181cb3e25

Plihal, W., & Born, J. (1997). Effects of early and late nocturnal sleep on declarative and procedural memory. *Journal of Cognitive Neuroscience*, *9*(4), 534–547. https://doi.org/10.1162/jocn.1997.9.4.534

Rajan, K. B., Weuve, J., Barnes, L. L., McAninch, E. A., Wilson, R. S., & Evans, D. A. (2021). Population estimate of people with clinical Alzheimer's disease and mild cognitive impairment in the United States (2020-2060). *Alzheimer's & Dementia: The Journal of the Alzheimer's Association*, *17*(12), 1966–1975. https://doi.org/10.1002/alz.12362

Reagh, Z. M., & Yassa, M. A. (2014). Object and spatial mnemonic interference differentially engage lateral and medial entorhinal cortex in humans. *Proceedings of the National Academy of Sciences*, *111*(40). https://doi.org/10.1073/pnas.1411250111

Reitan, R. M., & Wolfson, D. (1985). *The Halstead-Reitan neuropsychological test battery: Theory and clinical interpretation*. Neuropsychology Press.

Reitan, R. M., & Wolfson, D. (2001). The Halstead—Reitan Neuropsychological Test Battery: Research findings and clinical application. In A. S. Kaufman & N. L. Kaufman (Eds.), *Specific Learning Disabilities and Difficulties in Children and*

Adolescents (1st ed., pp. 309–346). Cambridge University Press. https://doi.org/10.1017/CBO9780511526794.011

Reuter, M., Rosas, H. D., & Fischl, B. (2010). Highly accurate inverse consistent registration: A robust approach. *NeuroImage*, *53*(4), 1181–1196. https://doi.org/10.1016/j.neuroimage.2010.07.020

Reuter, M., Schmansky, N. J., Rosas, H. D., & Fischl, B. (2012). Within-subject template estimation for unbiased longitudinal image analysis. *NeuroImage*, *61*(4), 1402–1418. https://doi.org/10.1016/j.neuroimage.2012.02.084

Roberts, R. O., Aakre, J. A., Kremers, W. K., Vassilaki, M., Knopman, D. S., Mielke, M. M., Alhurani, R., Geda, Y. E., Machulda, M. M., Coloma, P., Schauble, B., Lowe, V. J., Jack, C. R., & Petersen, R. C. (2018). Prevalence and outcomes of amyloid positivity among persons without dementia in a longitudinal, population-based setting. *JAMA Neurology*, *75*(8), 970–979. https://doi.org/10.1001/jamaneurol.2018.0629

Saeed, A., Lopez, O., Cohen, A., & Reis, S. E. (2023). Cardiovascular disease and Alzheimer's disease: The heart–brain axis. *Journal of the American Heart Association*, *12*(21), e030780. https://doi.org/10.1161/JAHA.123.030780

Saito, E. R., Warren, C. E., Hanegan, C. M., Larsen, J. G., du Randt, J. D., Cannon, M., Saito, J. Y., Campbell, R. J., Kemberling, C. M., Miller, G. S., Edwards, J. G., & Bikman, B. T. (2022). A novel ketone-supplemented diet improves recognition memory and hippocampal mitochondrial efficiency in healthy adult mice. *Metabolites*, *12*(11), 1019. https://doi.org/10.3390/metabo12111019

Scoville, W. B., & Milner, B. (1957). Loss of recent memory after bilateral hippocampal lesions. *Journal of Neurology, Neurosurgery, and Psychiatry*, *20*(1), 11–21.

Ségonne, F., Dale, A. M., Busa, E., Glessner, M., Salat, D., Hahn, H. K., & Fischl, B. (2004). A hybrid approach to the skull stripping problem in MRI. *NeuroImage*, *22*(3), 1060–1075. https://doi.org/10.1016/j.neuroimage.2004.03.032

Selkoe, D. J., & Hardy, J. (2016). The amyloid hypothesis of Alzheimer's disease at 25 years. *EMBO Molecular Medicine*, *8*(6), 595–608. https://doi.org/10.15252/emmm.201606210

Sled, J. G., Zijdenbos, A. P., & Evans, A. C. (1998). A nonparametric method for automatic correction of intensity nonuniformity in MRI data. *IEEE Transactions on Medical Imaging*, *17*(1), 87–97. https://doi.org/10.1109/42.668698

Tucker, M., Hirota, Y., Wamsley, E., Lau, H., Chaklader, A., & Fishbein, W. (2006). A daytime nap containing solely non-REM sleep enhances declarative but not procedural memory. *Neurobiology of Learning and Memory*, *86*(2), 241–247. https://doi.org/10.1016/j.nlm.2006.03.005

Villemagne, V. L., Burnham, S., Bourgeat, P., Brown, B., Ellis, K. A., Salvado, O., Szoeke, C., Macaulay, S. L., Martins, R., Maruff, P., Ames, D., Rowe, C. C., & Masters, C. L. (2013). Amyloid β deposition, neurodegeneration, and cognitive decline in sporadic Alzheimer's disease: A prospective cohort study. *The Lancet Neurology*, *12*(4), 357–367. https://doi.org/10.1016/S1474-4422(13)70044-9

Wilcoxon, F. (1945). Individual comparisons by ranking methods. *Biometrics Bulletin*, *1*(6), 80–83.

Wisse, L. E. M., Biessels, G. J., Heringa, S. M., Kuijf, H. J., Koek, D. (H.) L., Luijten, P. R., & Geerlings, M. I. (2014). Hippocampal subfield volumes at 7T in early Alzheimer's disease and normal aging. *Neurobiology of Aging*, *35*(9), 2039–2045. https://doi.org/10.1016/j.neurobiolaging.2014.02.021

Worsley, K. J., Taylor, J. E., Tomaiuolo, F., & Lerch, J. (2004). Unified univariate and multivariate random field theory. *NeuroImage*, *23 Suppl 1*, S189-195. https://doi.org/10.1016/j.neuroimage.2004.07.026

Zheng, W., Liu, H., Li, Z., Li, K., Wang, Y., Hu, B., Dong, Q., & Wang, Z. (2023). Classification of Alzheimer's disease based on hippocampal multivariate morphometry statistics. *CNS Neuroscience & Therapeutics*, *29*(9), 2457–2468. https://doi.org/10.1111/cns.14189

Zhu, D. C., Gwo, C., Deng, A., Scheel, N., Dowling, M. A., Zhang, R., & for the Alzheimer's Disease Neuroimaging Initiative. (2023). Hippocampus shape characterization with 3D Zernike transformation in clinical Alzheimer's disease progression. *Human Brain Mapping*, *44*(4), 1432–1444. https://doi.org/10.1002/hbm.26130

Appendix

Table S1

Hemispheric Brain Region and Memory Performance Correlations by Group

Group	Hemi	Structure	Episodic Learning		Episodic % Retention		Procedural Learning		Procedural % Retention	
			r [a]	*p*	r_s [b]	*p*	*r* [a]	*p*	r_s [b]	*p*
AD										
	Right	CA1	0.22	0.42	0.46	0.07	0.19	0.47	-0.16	0.55
		Subiculum	-0.11	0.70	0.01	0.96	0.14	0.61	-0.16	0.56
		Remainder	-0.48	0.06	-0.10	0.72	-0.25	0.36	-0.19	0.49
		Entorhinal	**0.61**	0.01	0.33	0.21	**0.50**	0.049	-0.30	0.26
	Left	CA1	0.40	0.13	**0.64**	0.01	0.16	0.55	-0.29	0.28
		Subiculum	0.03	0.91	0.04	0.88	0.12	0.66	0.10	0.72
		Remainder	-0.47	0.07	-0.35	0.19	-0.09	0.74	0.14	0.61
		Entorhinal	0.33	0.22	**0.57**	0.02	**0.52**	0.04	-0.45	0.08
aMCI										
	Right	CA1	**0.32**	0.04	0.28	0.07	0.03	0.87	-0.29	0.06
		Subiculum	0.19	0.23	0.11	0.48	**0.31**	0.04	-0.15	0.33
		Remainder	-0.09	0.56	-0.10	0.51	**0.31**	0.046	-0.02	0.87
		Entorhinal	-0.08	0.61	-0.11	0.48	0.07	0.66	-0.02	0.88
	Left	CA1	**0.43**	0.004	**0.35**	0.02	0.14	0.36	**-0.35**	0.02
		Subiculum	**0.35**	0.02	**0.33**	0.03	0.21	0.18	-0.27	0.08
		Remainder	**-0.30**	0.049	**-0.31**	0.04	0.17	0.28	0.02	0.89
		Entorhinal	0.01	0.94	**0.32**	0.04	0.08	0.62	0.04	0.82
CON										
	Right	CA1	0.23	0.47	-0.27	0.40	0.13	0.69	0.19	0.56
		Subiculum	-0.05	0.87	0.08	0.82	-0.19	0.56	0.24	0.46
		Remainder	0.00	1.00	-0.11	0.74	0.15	0.65	0.10	0.75
		Entorhinal	-0.28	0.38	0.40	0.20	-0.06	0.84	-0.28	0.38
	Left	CA1	0.04	0.90	-0.34	0.28	0.07	0.82	0.18	0.57
		Subiculum	-0.33	0.30	0.06	0.84	-0.06	0.84	0.08	0.82
		Remainder	-0.39	0.21	-0.39	0.21	0.26	0.42	-0.10	0.76
		Entorhinal	-0.04	0.90	0.17	0.60	-0.10	0.75	0.15	0.65

Note. Episodic scores are derived from CVLT-II performance. Procedural scores are derived from TMT-M performance.

[a] *r* = Pearson Correlation Coefficient. [b] r_s = Spearman Rank Correlations; used for percentage-based correlations.